**Supplementary information** is available on *Nature*'s World-Wide Web site (http://www.nature.com) or as paper copy from the London editorial office of *Nature*.

**Acknowledgements**

We thank E. C. Keystone for providing patient samples and C. Dunstan for critical comments. Technical assistance was provided by Y. Cheng, E. Julian, C. Burgh, A. Shahinian and D. Duryea. We are grateful to M. E. Saunders for scientific editing and A. Hessel, A. Oliveira dos Santos, K. Bachmaier, T. Sasaki and all other members of the laboratory for comments.

Correspondence and requests for materials should be addressed to J.M.P. (e-mail: jpenning@amgen.com).

# The p66$^{shc}$ adaptor protein controls oxidative stress response and life span in mammals

**Enrica Migliaccio*†, Marco Giorgio*†, Simonetta Mele‡, Giuliana Pelicci*, Paolo Reboldi§, Pier Paolo Pandolfi‖, Luisa Lanfrancone* & Pier Giuseppe Pelicci*‡**

** Department of Experimental Oncology, European Institute of Oncology, 20141 Milan, Italy*
*‖ Department of Human Genetics, Memorial Sloan-Kettering Cancer Center, Molecular Biology and Cell Biology Programs, Sloan-Kettering Institute, New York, New York 1021, USA*
*§ Istituto di Patologia Medica, Perugia University, 06100 Perugia, Italy*
*‡ Istituto di Medicina Interna e Scienze Oncologiche, Perugia University, 06100 Perugia, Italy*
*† These authors contributed equally to this work*

**Gene mutations in invertebrates have been identified that extend life span and enhance resistance to environmental stresses such as ultraviolet light or reactive oxygen species[1]. In mammals, the mechanisms that regulate stress response are poorly understood and no genes are known to increase individual life span. Here we report that targeted mutation of the mouse p66$^{shc}$ gene induces stress resistance and prolongs life span. p66$^{shc}$ is a splice variant of p52$^{shc}$/p46$^{shc}$ (ref. 2), a cytoplasmic signal transducer involved in the transmission of mitogenic signals from activated receptors to Ras[3]. We show that: (1) p66$^{shc}$ is serine phosphorylated upon treatment with hydrogen peroxide ($H_2O_2$) or irradiation with ultraviolet light; (2) ablation of p66$^{shc}$ enhances cellular resistance to apoptosis induced by $H_2O_2$ or ultraviolet light; (3) a serine-phosphorylation defective mutant of p66$^{shc}$ cannot restore the normal stress response in p66$^{shc-/-}$ cells; (4) the p53 and p21 stress response is impaired in p66$^{shc-/-}$ cells; (5) p66$^{shc-/-}$ mice have increased resistance to paraquat and a 30% increase in life span. We propose that p66$^{shc}$ is part of a signal transduction pathway that regulates stress apoptotic responses and life span in mammals.**

The mammalian proto-oncogene SHC locus encodes three proteins with relative molecular masses ($M_r$) of 52K(p52$^{shc}$), 46K(p46$^{shc}$) and 66K(p66$^{shc}$), which share a Src-homology2 (SH2) domain, a collagen-homology (CH1) region and a phosphotyrosine-binding (PTB) domain. p66$^{shc}$ contains a unique amino-terminal region (CH2; Fig. 1a)[2,3]. Like p52$^{shc}$/p46$^{shc}$, p66$^{shc}$ becomes tyrosine phosphorylated upon activation of growth factor receptors and forms stable complexes with Grb2, an adaptor protein for the Ras exchange factor SOS[2–5]. However, it does not affect mitogen-activated protein kinase (MAPK) activity and inhibits *c-fos* promoter activation[2], indicating that p66$^{shc}$ may not be involved in Ras activation. *c-fos* is transcriptionally activated in response to environmental stresses such as DNA-damaging agents (for example, ultraviolet light (UV)) or agents that induce oxidative damage by increasing intracellular levels of reactive oxygen species (ROS) (such as $H_2O_2$)[6].

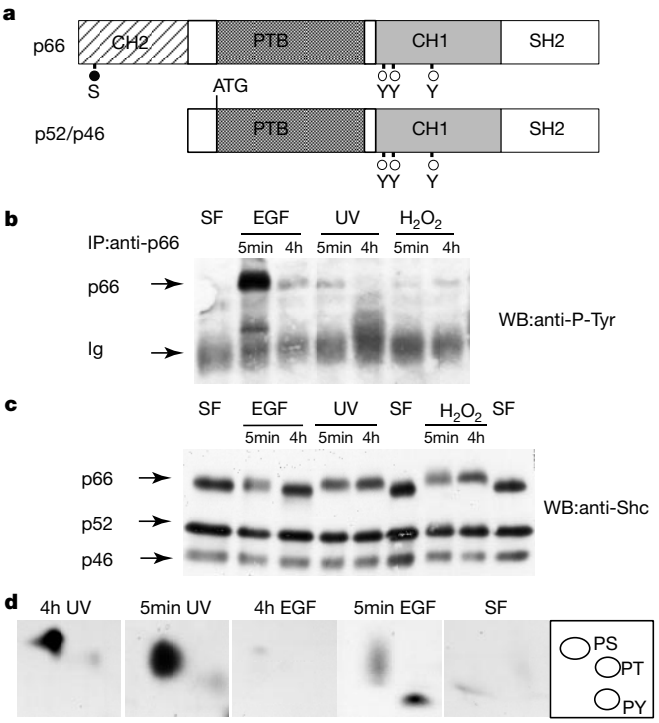


**Figure 1** Serine phosphorylation of p66$^{shc}$ by oxidative damage. **a**, Organization of Shc proteins. p66$^{shc}$ and p52$^{shc}$/p46$^{shc}$ are encoded by two distinct transcripts that differ in the use of 5′ coding exons[2]. S: S36, the major serine-phosphorylation site of p66$^{shc}$; Y: tyrosine-phosphorylation sites. **b**, Tyrosine phosphorylation of p66$^{shc}$. Anti-p66 immunoprecipitates (IP) from starved or EGF, $H_2O_2$ or UV-treated MEFs were blotted (WB) with anti-phosphotyrosine (anti-P-Tyr) antibodies. Ig: immunoglobulin cross-reactive polypeptides. **c**, Western blot analysis of Shc expression. Lysates from serum starved (SF) or treated MEFs were probed with anti-Shc antibodies. **d**, Phospho-amino-acid analysis of p66$^{shc}$. Serum-starved MEFs were labelled with [$^{32}$P]orthophosphate (SF) and treated with EGF or UV for 5 min or 4 h. Phospho-amino-acid analysis was performed on the immunoprecipitated p66$^{shc}$ polypeptides. Positions of phosphoserine (PS), phosphothreonine (PT) and phosphotyrosine (PY) markers are indicated.

To investigate the role of p66$^{shc}$ in stress responses, we analysed the extent of its tyrosine phosphorylation in mouse embryo fibroblasts (MEFs) treated with UV, $H_2O_2$ or epidermal growth factor (EGF). EGF, but not UV or $H_2O_2$, induced tyrosine phosphorylation of p66$^{shc}$, which was maximal after 5 min (Fig. 1b). However, UV and $H_2O_2$ provoked marked gel retardation of p66$^{shc}$ (Fig. 1c), indicating other possible post-translational modifications. Phospho-amino-acid analysis of p66$^{shc}$ phosphorylation after treatment with UV (Fig. 1d) or $H_2O_2$ (data not shown) revealed a marked and persistent (up to 4 h) increase in phosphoserine. It appears, therefore, that p66$^{shc}$ is involved in the cellular responses to both growth factors and environmental stresses; possibly through distinct pathways, as EGF induced phosphorylation on tyrosine, whereas UV or $H_2O_2$ induced phosphorylation on serine.

To investigate the function of p66$^{shc}$ in the environmental stress response, we analysed the effects of ablation of p66$^{shc}$ on the cellular response to oxidative ($H_2O_2$) or DNA (UV or γ-irradiation) damage. MEFs were derived from mice carrying a targeted mutation of the *Shc* CH2 exon, which did not affect p52$^{shc}$/p46$^{shc}$ coding sequences (M.G. *et al.*, in preparation). As expected, p66$^{shc}$ was reduced in p66$^{shc+/-}$ and absent in p66$^{shc-/-}$ MEFs, whereas p52$^{shc}$/

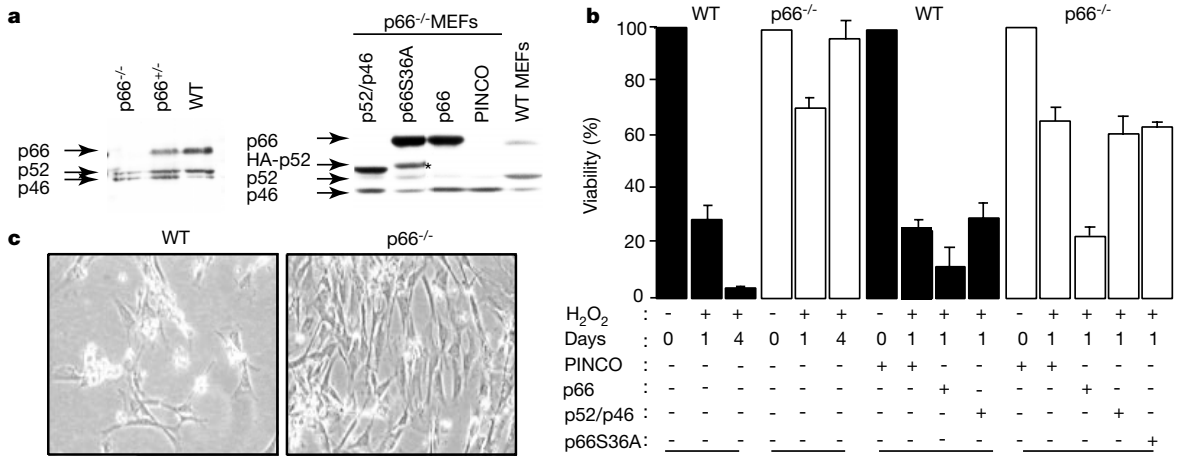


**Figure 2** Targeted mutation of p66$^{shc}$ induces cellular resistance to oxidative damage. **a**, Anti-Shc western blots of wild-type (WT), p66$^{shc+/-}$ or $^{-/-}$ MEFs (left) and of p66$^{shc-/-}$ MEFs infected with PINCO or PINCO retroviruses expressing p66$^{shc}$, p52$^{shc}$/p46$^{shc}$ or p66$^{shc}$S36A cDNAs (right). **b**, Viability of MEFs after $H_2O_2$ treatment. Wild-type and p66$^{shc-/-}$ MEFs were treated with $H_2O_2$ for 1 or 4 days, as indicated. In separate experiments, cells were infected with PINCO or with PINCO retroviruses expressing the p66$^{shc}$, p52$^{shc}$/46$^{shc}$ or p66S36A cDNAs, kept for 48 h to allow gene expression of exogenous cDNAs and treated with $H_2O_2$. Cell viability was determined by trypan blue exclusion. Results are expressed as percentage of viable cells with respect to untreated controls and represent the mean of triplicate cultures. This experiment is representative of four that gave similar results. **c**, Morphology of wild-type and p66$^{shc-/-}$ MEFs 24 h after $H_2O_2$ treatment (original magnification 100×).

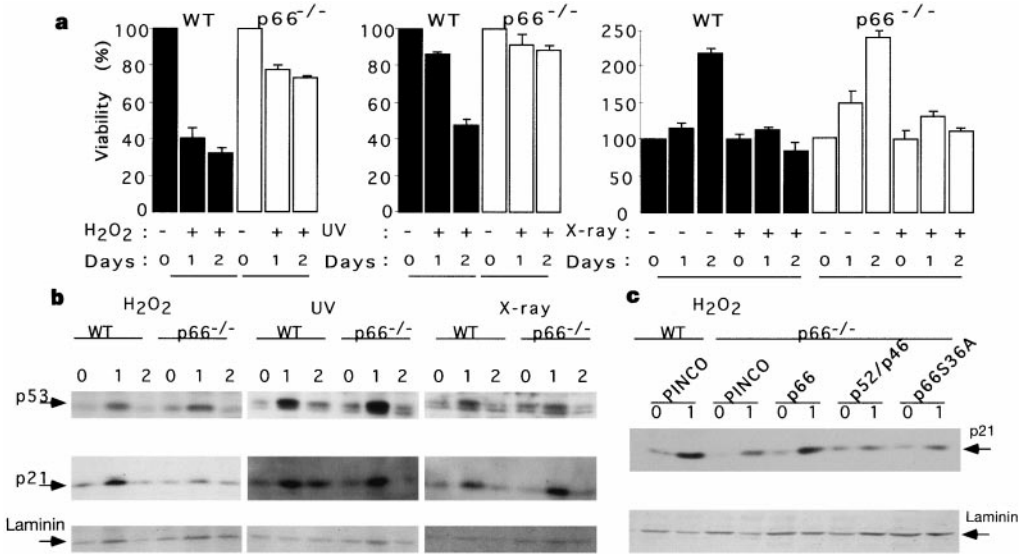


**Figure 3** p53 and p21 regulation in p66$^{shc-/-}$ MEFs after $H_2O_2$, UV and X-rays. **a**, MEFs were treated with $H_2O_2$, UV or X-rays and evaluated by trypan blue exclusion. **b**, Western blot analysis of p53, p21 and laminin expression in wild-type and p66$^{shc-/-}$ MEFs after $H_2O_2$, UV and X-rays. The cellular lysates were derived from the experiment shown in **a**. **c**, Western blot analysis of p21 and laminin expression in PINCO-infected wild-type MEFs and in p66$^{shc-/-}$ cells after infection with PINCO retroviruses expressing p66$^{shc}$, p52$^{shc}$/p46$^{shc}$ or p66S36A.

p46$^{shc}$ was detectable in both (Fig. 2a, left). Wild-type (WT) MEFs were sensitive to $H_2O_2$, with 70% of cells dying after one day of treatment (Fig. 2b, c). *In situ* terminal deoxynucleotidyl transferase assay revealed massive apoptosis (>70%; data not shown). Overexpression of p66$^{shc}$ increased the susceptibility of wild-type MEFs (85–90% cell death; Fig. 2b), whereas p66$^{shc}$ ablation increased resistance of MEFs to $H_2O_2$ (<30% cell death; Fig. 2b, c). p66$^{shc-/-}$ MEFs that survived oxidative stress maintained their proliferative potential, as revealed by their ability to restore the initial cell number within a few days (Fig. 2b). Similar results were obtained by treating cells with UV: in wild-type MEFs, about 80% and 40% of the cells survived after one and two days of treatment, respectively, whereas in the p66$^{shc-/-}$ MEFs the cytotoxic effect of UV was negligible (Fig. 3a). Apoptosis after one day of treatment was 20–25% and 5–7.5% in wild-type and p66$^{shc-/-}$ MEFs, respectively (data not shown). Expression of p66$^{shc}$, but not p52$^{shc}$/p46$^{shc}$, into p66$^{shc-/-}$ cells restored a normal response to $H_2O_2$ (Fig. 2a, b) and UV (data not shown). γ-Irradiation, in contrast, induced arrest of cell proliferation (G1 arrest; data not shown) without significant loss of cell viability (Fig. 3a) in wild-type and p66$^{shc-/-}$ MEFs. UV and X-rays induce DNA damage; only UV, however, increases intracellular ROS and induces oxidative damage, which is the main causative agent in the physiological response to UV[7]. It appears, therefore, that p66$^{shc}$ is a crucial component of the apoptotic response to oxidative damage, whereas it has no effect on the arrest of cell proliferation induced by DNA damage.

Activation of serine-threonine kinases is a prominent feature of the response to oxidative damage ($H_2O_2$ or UV)[8]. To test whether $p66^{shc}$ is a cytoplasmic transducer of oxidative stress signals, we evaluated the biological activity of a serine-phosphorylation mutant of $p66^{shc}$. The isolated $p66^{shc}$ CH2 region, expressed in fibroblasts, exhibited gel retardation upon treatment with EGF or $H_2O_2$, suggesting modifications of phosphoserine-type (Fig. 4a, top). Alanine substitution of the CH2 serine 36 (S36A) abrogated the $H_2O_2$-induced gel-mobility shift of both the isolated CH2 polypeptide (Fig. 4a, middle) and of the full-length $p66^{shc}$ (Fig. 3a, bottom), and markedly reduced serine phosphorylation of $p66^{shc}$ upon $H_2O_2$ treatment (Fig. 4b). Expression of the p66S36A mutant into $p66^{shc-/-}$ MEFs (Fig. 2a, right) did not restore a normal response to $H_2O_2$ (Fig. 2b). It appears, therefore, that serine phosphorylation of $p66^{shc}$ is critical for the activation of apoptosis in cells exposed to oxidative damage. $p66^{shc}$ might monitor the intracellular concentration of ROS and eliminate cells injured by oxidative damage.

The cellular stress response involves upregulation of the tumour suppressor p53 and the cyclin-dependent kinase inhibitor p21, a transcriptional target of p53 (ref. 9). The p21 response to UV or $H_2O_2$ is regulated through both p53-dependent and -independent pathways, whereas p21 upregulation by X-rays depends only on p53 activation[10–12]. We investigated the regulation of p53 and p21 by $H_2O_2$, UV and X-rays in wild-type and $p66^{shc-/-}$ MEFs. Upregulation of p53 was comparable in wild-type and $p66^{shc-/-}$ cells (Fig. 3b). However, upregulation of p21 was significantly reduced in the $p66^{shc-/-}$ cells following treatment with $H_2O_2$ and UV, but not X-rays (Fig. 3b), indicating that $p66^{shc}$ interferes with p53-independent pathway(s) that control p21 upregulation following oxidative damage. Overexpression of $p66^{shc}$, but not of p66S36A or $p52^{shc}$/$p46^{shc}$, restored the normal p21 response to oxidative stress in $p66^{shc-/-}$ cells (Fig. 3c). To test the role of p21 in the increased stress resistance of $p66^{shc-/-}$ cells, we overexpressed p21 in wild-type and $p66^{shc-/-}$ cells. Overexpression of p21 protected wild-type MEFs from $H_2O_2$-induced cell death and did not abrogate the survival

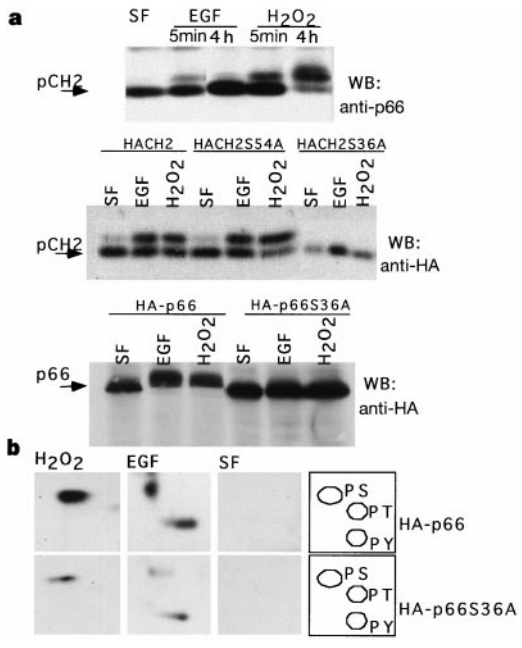


**Figure 4** Mapping of $p66^{shc}$ serine-phosphorylation sites. **a**, Wild-type MEFs were transfected with expression vectors for haemagglutinin (HA)-tagged versions of wild-type (top), S54A or S36A (middle) CH2 polypeptides, $p66^{shc}$ or p66S36A (bottom). Serum-starved (SF) cells were treated with EGF or $H_2O_2$ and analysed by western blotting using anti-p66 or anti-HA antibodies, as indicated. **b**, Phospho-amino-acid analysis of HA–$p66^{shc}$ and HA–p66S36A.

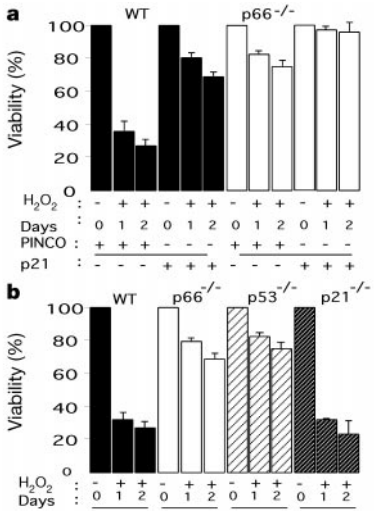


**Figure 5** Effects of p21 expression on the oxidative stress response of wild-type and $p66^{shc-/-}$ cells. **a**, Wild-type and $p66^{shc-/-}$ MEFs were infected with PINCO or with PINCO retrovirus expressing p21 and treated with $H_2O_2$. Cell viability was determined after 1 or 2 days by trypan blue exclusion. This experiment is representative of two that gave similar results. **b**, Viability of wild-type, $p66^{shc-/-}$, $p53^{-/-}$ and $p21^{-/-}$ MEFs after exposure to $H_2O_2$.

effect of $p66^{shc}$ ablation (Fig. 5a). $p21^{-/-}$ MEFs had a normal oxidative stress response, whereas $p53^{-/-}$ MEFs were resistant (Fig. 5b)[13,14]. It appears, therefore, that the apoptotic response to oxidative stress is mediated by p53 and antagonized by p21. Together, these findings indicate that oxidative stress may activate two pathways: one involving p53 and leading to apoptosis, and the other involving p21, through p53-dependent and -independent mechanisms, and protecting from apoptosis. Ablation of $p66^{shc}$ interrupts both pathways of p21 upregulation and p53-dependent apoptosis induced by oxidative stress.

To examine the ability of $p66^{shc-/-}$ mice to resist oxidative stress *in vivo*, animals were treated with paraquat, with generates superoxide anions upon cellular intake[15]. Ten mice of ten weeks of age were injected intraperitoneally with 70 mg $kg^{-1}$ paraquat. All of the five wild-type mice died within 48 h, whereas, of the five injected $p66^{shc-/-}$ mice, two died within the first 48 h, two died within 72 h and one survived for several weeks. The same experiment was repeated using five wild-type and five $p66^{shc-/-}$ mice of nine weeks of age, with comparable results. Cumulative statistical analysis revealed a 40% increase in the mean survival time of the $p66^{shc-/-}$ mice over the wild type (67.4 ± 6.7 and 44.8 ± 4.6 h, respectively; $P = 0.0109$) (Fig. 6a). These results indicate that ablation of $p66^{shc}$ expression enhances resistance to oxidative stress *in vivo*.

Enhanced resistance to environmental stress correlates with increased life span in invertebrates. In *Saccharomyces cerevisiae*, deletions of *RAS1* (ref. 16) or mutations in the *SIR4* (ref. 17) locus increase life span and stress resistance. In *Caenorhabditis elegans*, mutants of *clk-1* and of the genes of the dauer/insulin receptor signalling pathway (*daf-2*; *age-1*, *AKT1* and *AKT-2*; *PDK1*) survive longer and are more resistant to ROS, heat and UV[18,19]. In *Drosophila melanogaster*, selection for late-life fitness is associated with greater resistance to environmental stresses[20], and hypomorphic mutants of the *mth* locus live 35% longer and are more resistant to dietary paraquat and starvation[21]. A few progeric mutations have been described in *C. elegans* (Mev-1) and *Drosophila* (catalase or SOD), and, in all cases, decreased life span correlates with enhanced sensitivity to oxidative stress[22,23]. We conducted a prospective observational study to evaluate the effects

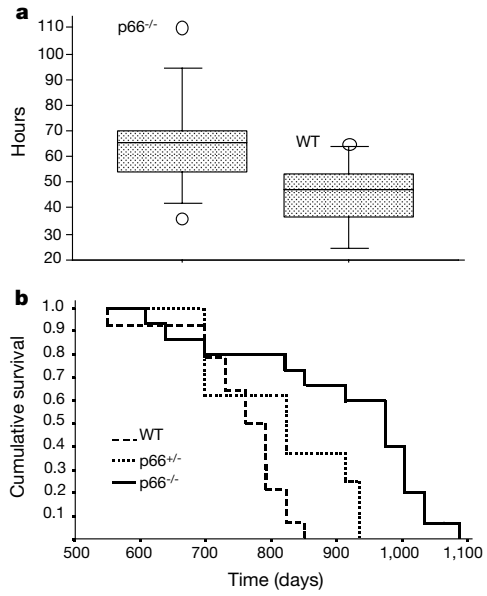


**Figure 6** Increased resistance to oxidative stress and prolonged life span of p66$^{shc-/-}$ mice. **a**, 10 wild-type and 10 p66$^{shc-/-}$ mice were treated with paraquat in two separate experiments. In the first, paraquat was administered to 5 wild-type and 5 p66$^{shc-/-}$ mice of 10 weeks of age; in the second, to 5 wild-type and 5 p66$^{shc-/-}$ mice of 9 weeks of age. Cumulative statistical analysis (two-way analysis of variance) revealed representation of the mean survival time (h) of the wild-type and p66$^{shc-/-}$ mice in a box and whisker plot is shown. **b**, Cumulative survival (Kaplan and Meier) of wild-type, p66$^{shc+/-}$ and p66$^{shc-/-}$ mice.

of the p66$^{shc}$ mutation on mouse survival. Thirty-seven mice born in August 1996 from p66$^{shc+/-}$ heterozygous parents were not sacrificed and were maintained under identical conditions. There were 14 wild-type, 8 p66$^{shc+/-}$ and 15 p66$^{shc-/-}$ mice. After 28 months, when all the wild-type animals had died, three of the eight heterozygous (37%) and 11 of the 15 homozygous mice (73%) were still alive. The remaining three p66$^{shc+/-}$ and 11 p66$^{shc-/-}$ mice died after a further two and eight months, respectively. Comparison of survival curves by the Kaplan and Meier method[24] showed a highly significant difference among the three groups (log-rank 16.72; $P = 0.0002$), with median survivals of 761 ± 19.02 days (wild type), 815.38 ± 37.46 (p66$^{shc+/-}$) and 973 ± 37.31 (p66$^{shc-/-}$) (Fig. 6b). Comparison of survival curves of wild-type versus p66$^{shc-/-}$ mice showed an ~30% increase in life span of the p66$^{shc-/-}$ mice (log-rank 13.29; $P = 0.0003$). Differences in the cumulative survival of the wild-type versus p66$^{shc+/-}$ group, however, did not reach full statistical significance (log-rank 3.62; $P = 0.057$). The only other known model of increased life span in mammals is food restriction, which, in rodents, increases mean and maximum survival times[25,26]. However, no statistically significant differences were found in body weight and food consumption of the p66$^{shc-/-}$ mice. Phenotypical and histopathological analysis revealed no obvious abnormalities in the p66$^{shc-/-}$ mice (see Supplementary Information). In conclusion, it appears that homozygous mutation of p66$^{shc}$ increases life span in mice, in the absence of any obvious defective phenotype.

Among currently accepted evolutionary theories, it is postulated that ageing is a post-reproductive process which has escaped the force of natural selection and which evolved through selection of alleles with early life benefits combined with pleiotropically harmful effects later in life[27]. The postulated genes, as they would be actively selected, are expected to regulate fundamental cellular processes common to different species. Accumulation of oxidative cellular damage, inflicted by ROS, is the major proximal cause of ageing in both invertebrates and mammals. Cellular defences against oxidative damage exist (catalase and Cu/Zn superoxide dismutase, SOD); however, they are not completely efficient, as oxidatively damaged macromolecules accumulate in virtually all ageing organisms examined[28]. In *C. elegans* and *Drosophila*, there is evidence that genes controlling ROS metabolism determine life span and that decreased ROS production might be responsible for elevated resistance to oxidative stress and increased longevity[23,29]. In mammals, restriction of caloric intake lowers steady-state levels of oxidative stress and damage and extends the maximum life span[30]. p66$^{shc}$ is part of a signal transduction pathway that is activated by increased intracellular ROS and which leads to apoptosis. Mutation of this pathway increases cellular and organism oxidative stress resistance and life span. Biochemical and genetic investigation of the p66$^{shc}$ signalling pathway should lead to better understanding of the control mechanisms and relationships between ROS metabolism, cellular survival and organism ageing in mammals. □

## Methods

### Cells, plasmids and antibodies

MEFs derived from wild-type 129, p66$^{shc+/-}$ and $^{-/-}$, p53$^{-/-}$ (from A. R. Clarke), and p21$^{-/-}$ (from M. Serrano) mice were treated with 30 ng ml$^{-1}$ EGF or 400 μM $H_2O_2$, or irradiated with 10 J m$^{-2}$ UV-C (254 nm) or 5 Gy X-rays. The p21, p52$^{shc}$-p46$^{shc}$, p66$^{shc}$, p66$^{shc}$S36A, haemagglutinin (HA)–CH2, HA–CH2S35A, HA–CH2S54A, HA–p66$^{shc}$, HA–p66$^{shc}$-S36A and HA–p66$^{shc}$S54A complementary DNAs were cloned into the pCDNA3 or PINCO expression vectors. The anti-Shc and anti-p66$^{shc}$ polyclonal antibodies recognize the SH2 domain of all three Shc isoforms and the CH2 region, respectively[2,3]. The anti-HA, anti-lamin B (Ab1), anti-p53 (CM5) and anti-p21 (F5) antibodies were purchased from Oncogene Research Products, Novo Castra and Santa Cruz, respectively.

### Metabolic labelling and phospho-amino-acid analysis

Serum-starved cells were labelled for 4 h in phosphate-free DMEM containing 0.5% FBS and 1 mCi ml$^{-1}$ [$^{32}$P]orthophosphate, treated with EGF, $H_2O_2$ or UV and lysed, p66$^{shc}$ proteins were immunoprecipitated, resolved by SDS–PAGE, transferred to PVDF membranes and hydrolysed in 6 M HCl for 60 min at 110 °C. The hydrolysis products were separated in the presence of phosphoserine, phosphothreonine and phosphotyrosine markers by SDS–PAGE at pH = 1.9 and pH = 3.5 in two dimensions on TLC plates.

### Transfections and infections

MEFs were transfected with the LipofectaMINE PLUS Reagent GibcoBRL (averaged transfection efficiency 50%). For retrieval infections, we used the PINCO vector, which expresses the green fluorescence protein (GFP) cDNA from an internal cytomegalovirus promoter. The efficiency of infection (~80%) was determined by FACS analysis of GFP-positive cells 48 h after infection.

### Paraquat experiments

The wild-type and p66$^{shc-/-}$ mice are carriers of mouse hepatitis virus and free of other common viral agents (Sendai, Pneumonia and Mycoplasma). Animals were maintained under a 12 h light–12 h dark cycle and given food and water *ad libitum*. For paraquat experiments, 10 wild-type and 10 p66$^{shc-/-}$ male mice were injected intraperitoneally with 70 mg kg$^{-1}$ paraquat in PBS.

Received 21 July; accepted 8 September 1999.

1. Martin, G. M., Austad, S. N. & Johnson, T. E. Genetic analysis of aging: role of oxidative damage and environmental stresses. *Nature Genet.* **13,** 25–34 (1996).
2. Migliaccio, E. *et al.* Opposite effects of the p52$^{shc}$/p46$^{shc}$ splicing isoforms on the EGF receptor-MAP kinase-fos signaling pathway. *EMBO J.* **16,** 706–716 (1997).
3. Pelicci, G *et al.* A novel transforming protein (SHC) with a SH2 domain is implicated in mitogenic signal transduction. *Cell* **70,** 93–104 (1992).
4. Bonfini, L., Migliaccio, E., Pelicci, G., Lanfrancone, L. & Pelicci, P. G. Not all Shc's roads lead to Ras. *Trends Biochem. Sci.* **21,** 257–261 (1996).
5. Rozakis-Adcock, M. *et al.* Association of the Shc and Grb2/Sem5 SH2-containing proteins is implicated in activation of the Ras pathway by tyrosine kinase. *Nature* **360,** 689–692 (1992).
6. Sen, C. & Packer, L. Antioxidant and redox regulation of gene transcription. *FASEB J.* **10,** 709–720 (1996).
7. Renzing, J., Hansen, S. & Lane, D. P. Oxidative stress is involved in the UV activation of p53. *J. Cell Sci.* **109,** 1105–1112 (1996).
8. Stevenson, M. A., Pollock, S. S., Coleman, C. N. & Calderwood, S. K. X-irradiation, phorbol esters, and $H_2O_2$ stimulate mitogen-activated protein kinase activity in NiH-3T3 cells through the formation of reactive oxygen intermediates. *Cancer Res.* **54,** 12–15 (1994).
9. Lu, X. & Lane, D. P. Differential induction of transcriptionally active p53 following UV or ionizing radiation: defects in chromosome instability syndromes? *Cell* **75,** 765–778 (1993).
10. Deng, C., Zhang, P., Harper, J. W., Elledge, S. J. & Leder, P. Mice lacking p21CIP/WAF1 undergo normal development, but are defective in G1 checkpoint control. *Cell* **82,** 675–684 (1995).
11. Russo, T. *et al.* A p53-independent pathway for activation of WAF1/C1P1 expression following oxidative stress. *J. Biol. Chem.* **270,** 29386–29391 (1995).

12. Macleod, K. F. *et al.* p53-dependent and independent expression of p21 during cell growth, differentiation, and DNA damage. *Genes Dev.* **9,** 935–944 (1995).
13. Yin, Y., Solomon, G., Deng, C. & Barrett, J. C. Differential regulation of p21 by p53 and Rb in cellular response to oxidative stress. *Mol. Carcin.* **24,** 15–24 (1999).
14. Yin, Y. *et al.* Involvement of p85 in p53-dependent apoptotic response to oxidative stress. *Nature* **391,** 707–710 (1998).
15. De Haan j., B. *et al.* Mice with a homozygous null mutation for the most abundant glutathione peroxidase, Gpx1, show increased susceptibility to the oxidative stress-inducing agents paraquat and hydrogen peroxide. *J. Biol. Chem.* **273,** 22528–22536 (1998).
16. Sun, J., Childress, A. M., Pinswasdl, C. & Jazwinski, S. Divergent roles of RAS1 and RAS2 in yeast longevity. *J. Biol. Chem.* **269,** 18638–18645 (1994).
17. Kennedy, B. K., Austriaco, N. R., Zhang, J. & Guarente, L. Mutation in the silencing gene SIR4 can delay aging in *S. cerevisiae. Cell* **80,** 485–496 (1995).
18. Murakami, S. & Johnson, T. E. A genetic pathway conferring life extension and resistance to UV stress in *Caenorhabditis elegans. Genetics* **143,** 1207–1218 (1996).
19. Larsen, P. L., Albert, P. S. & Riddle, D. L. Genes that regulate both development and longevity in *C. elegans. Genetics* **139,** 1576–1583 (1995).
20. Service, P. M., Hutchinson, E. W., MacKinley, M. D. & Rose, M. R. Resistance to environmental stress in *Drosophila melanogaster* selected for postponed senescence. *Physiol. Zool.* **58,** 380–389 (1985).
21. Lin, Y. J., Seroude, L. & Benzer, S. Extended life-span and stress resistance in the *Drosophila* mutant *methuselah. Science* **282,** 943–946 (1998).
22. Ishi, N. *et al.* A mutation in succinate dehydrogenase cytochrome b causes oxidative stress and ageing in nematodes. *Nature* **394,** 694–697 (1998).
23. Orr, W. C. & Sohal, R. S. Extension of life-span by overexpression of superoxide dismutase and catalase in *D. melanoganster. Science* **263,** 1128–1130 (1994).
24. Marubini, E. & Valsecchi, M. G. *Analysing Survival Data from Clinical Trials and Observational Studies* (Wiley, New York, 1995).
25. Weindruch, R., Walford, R. L., Fligiel, S. & Guthetrie, D. The retardation of aging in mice by dietary restriction: longevity, cancer, immunity and lifetime energy intake. *J. Nutr.* **116,** 641–654 (1986).
26. Weindruch, R. & Walford, R. L. Dietary restriction in mice beginning at 1 year of age: effect on life-span and spontaneous cancer incidence. *Science* **215,** 1415–1417 (1982).
27. Medawar, P. B. Old age and natural death. *Modern Quarterly* **1,** 30–56 (1946).
28. Lithgow, G. J. & Kirkwood, T. B. L. Mechanisms and evolution of aging. *Science* **273,** 80 (1996).
29. Taub, J. *et al.* A cytosolic catalase is needed to extend adult life span in C. *elegans daf-C* and *clk*-1 mutants. *Nature* **399,** 162–166 (1999).
30. Sohal, R. S. & Weindruch, R. Oxidative stress, caloric restriction, and aging. *Science* **273,** 59–63 (1996).

**Supplementary Information** is available on *Nature*'s World-Wide Web site (http://www.nature.com) or as paper copy from the London editorial office of *Nature*.

**Acknowledgements**

We thank V. Soares, P. P. DiFiore, K. Helin, L. Bonfini, I. Nicoletti and G. Della Porta for discussions; C. Matteucci, C. Casciari, M. Scanarini and G. Pelliccia for technical help; A. Ventura and A. Cicalese for contributions; and A. Ariesi for secretarial work. We also acknowledge continuous technical and intellectual support from L. Pozzi in conducting animal experiments. E.M. is the recipient of a fellowship from FIRC. This work was supported by A.I.R.C.

Correspondence and requests for materials should be addressed to P.G.P. (e-mail: pgpelicci@ieo.it).

# Structural insights into phosphoinositide 3-kinase catalysis and signalling

**Edward H. Walker*, Olga Perisic*, Christian Ried*, Len Stephens† & Roger L. Williams***

* *MRC Laboratory of Molecular Biology, MRC Centre, Hills Road, Cambridge CB2 2QH, UK*
† *The Babraham Institute, Babraham, Cambridge CB2 4AT, UK*

**Phosphoinositide 3-kinases (PI3Ks) are ubiquitous lipid kinases that function both as signal transducers downstream of cell-surface receptors and in constitutive intracellular membrane and protein trafficking pathways. All PI3Ks are dual-specificity enzymes with a lipid kinase activity which phosphorylates phosphoinositides at the 3-hydroxyl, and a protein kinase activity. The products of PI3K-catalysed reactions, phosphatidylinositol 3,4,5-trisphosphate (PtdIns(3,4,5)$P_3$), PtdIns(3,4)$P_2$ and PtdIns(3)P, are second messengers in a variety of signal transduction pathways, including those essential to cell proliferation, adhesion, survival, cytoskeletal rearrangement and vesicle trafficking[1,2]. Here we report the 2.2 Å X-ray crystallographic structure of the catalytic subunit of PI3Kγ, the class I enzyme that is activated by heterotrimeric G-protein βγ subunits and Ras. PI3Kγ has a modular organization centred around a helical-domain spine, with C2 and catalytic domains positioned to interact with phospholipid membranes, and a Ras-binding domain placed against the catalytic domain where it could drive allosteric activation of the enzyme.**

The mammalian PI3Ks can be divided into three classes on the basis of their structure and substrate specificity[2]. The class I PI3Ks are receptor-regulated heterodimeric enzymes that preferentially phosphorylate PtdIns(4,5)$P_2$ *in vivo*. The class IA PI3Ks (consisting of p110α, p110β or p110δ catalytic subunits) associate with a p85 adaptor protein that is essential for interaction of these PI3Ks with receptor tyrosine kinases. The class IB PI3K (PI3Kγ) is activated by heterotrimeric G-protein subunits and associates with a p101 adaptor that is required for full responsiveness to Gβγ heterodimers[3,4]. Class I PI3Ks are also activated by Ras. Class II PI3Ks are distinguished by a carboxy-terminal C2 domain and preferentially use PtdIns and PtdIns(4)P as substrates. Class III enzymes phosphorylate only PtdIns and lack the Ras-binding domain.

We have determined the structure of the catalytic subunit (residues 144–1,102) of porcine PI3Kγ. This construct contains all of the homology regions (HR) found in class I PI3Ks (HR1, HR2, HR3 and HR4) and has a catalytic activity similar to that of the full-length enzyme. The amino-terminal region missing from our construct of PI3Kγ is important for interaction with the p101 adaptor[5], and the analogous region of PI3Kα interacts with the p85 adaptor. The enzyme has a modular structure consisting of four domains: a Ras-binding domain (RBD), a C2 domain, a helical domain and a catalytic domain (Fig. 1). The RBD, C2 and catalytic domains have folds similar to these modules in other proteins involved in signal transduction. The helical domain has a fold akin to HEAT repeat containing structures involved in protein–protein interactions.

The catalytic domain of the enzyme consists of a smaller N-terminal lobe (residues 726–883) and a larger C-terminal lobe (884–1092). The N-terminal lobe from kβ3 to kα3 and the first part of the C-terminal lobe (up to the end of kβ10) have a fold similar to protein kinases (reviewed in ref. 6), and this similarity extends to many of the details of the ATP-binding site (Fig. 2). This region is among the most conserved regions of the PI3Ks (Fig. 3). The structural similarity of PI3K to protein kinases is consistent with PI3Ks having protein kinase activity in addition to their lipid kinase activities[7,8]. The sequence alignment in Fig. 3 shows the regions of PI3K that structurally superimpose with tyrosine protein kinase c-Src. The N-terminal lobe comprises a five-stranded anti-parallel β-sheet flanked on one side by a helical hairpin (kα1–kα2) and a small two-stranded β-sheet (β1–β2), and on the other side by the kα3 helix and the C-terminal lobe. Strands kβ3–kβ7 correspond to the five-stranded β-sheet found in the protein kinases. The kβ3–kβ4 loop corresponds to the protien kinase β1–β2 loop (also known as the glycine-rich or P-loop). This loop interacts closely with the phosphates of the bound ATP, but unlike the protein kinases, it contains no glycine. Instead, the side chain of Ser 806, a residue that is conserved in all PI3Ks, interacts with the β-phosphate (Fig. 2). Lys 833 at the end of kβ5, corresponding to Lys 72 of c-AMP-dependent protein kinase, interacts with the α-phosphate of ATP. This residue is conserved in all PI3Ks and is covalently modified by wortmannin[9]. There are two metal-binding sites (Me; Fig. 2). Me I interacts with the conserved Asn 951, whereas Me II interacts with Asp 836 and Asp 964.

N- and C-terminal lobes are linked through a loop between strands kβ7 and kβ8. This loop forms the deepest wall of the ATP-